

# Reduced basis methods for optimal control of advection-diffusion problems\*

Alfio Quarteroni<sup>‡,§</sup>, Gianluigi Rozza<sup>§</sup>, Annalisa Quaini<sup>§</sup>

January 30, 2006

<sup>‡</sup> MOX– Modellistica e Calcolo Scientifico  
Dipartimento di Matematica “F. Brioschi”  
Politecnico di Milano  
via Bonardi 9, 20133 Milano, Italy

`alfio.quarteroni@mate.polimi.it`

<sup>§</sup> Modeling and Scientific Computing, IACS-CMCS  
École Polytechnique Fédérale de Lausanne, EPFL  
Station 8, CH-1015 Lausanne, Switzerland

`{alfio.quarteroni, gianluigi.rozza, annalisa.quaini}@epfl.ch`

*Dedicated to Yuri Kuznetsov for his 60<sup>th</sup> birthday.*

**Keywords:** advection-diffusion parametrized partial differential equations, reduced-basis methods, Galerkin approximation, optimal control, geometrical sensitivity analysis, environmental fluid dynamics.

**AMS Subject Classification:** 49J20, 76R50, 76B75.

## Abstract

The reduced basis (RB) method is proposed for the approximation of multi-parametrized equations governing an optimal control problem. The idea behind the RB method is to project the solution onto a space of small dimension, specifically designed on the problem at hand, and to decouple the generation and projection stages (off-line/on-line computational procedures) of the approximation process in order to solve parametrized equations in a rapid and not expensive way.

The application that we investigate is an air pollution control problem: we aim at regulating the emissions of industrial chimneys in order to keep the pollutant concentration below a certain threshold over an observation area, like a town. Adopting the RB method for both state and adjoint equations

---

\*This work has been supported by Italian MIUR Cofin2003 “Numerical modeling for scientific computing and advanced applications”, EPFL and Swiss National Science Foundation.

of the optimal control problem leads to important computational savings with respect to the use of the Galerkin-finite element method. We consider different parametrization (control, physical and geometrical input parameters) so that we are able to solve the control problem from a global and decisional point of view.

## 1 Introduction

The control and optimization of an engineering component or system requires the prediction of certain “quantities of interest”, which we shall generically call *outputs*. They are typically expressed as functionals of the field variables (either state or adjoint variable) associated with a partial differential equation which describes the physical behavior of the component or the system. The parameters, which we shall denote *inputs*, identify a particular “configuration” of the components: they may represent variables related to the control function  $u$ , but also physical or geometrical parameters. We thus get an implicit *input-output* relationship whose evaluation requires the solution of the underlying partial differential equations.

Generically speaking, the solution of control problems requires *rapid*, *reliable*, and *repeated* evaluations of the input-output relationship. This calls for methods that can reduce complexity while preserving all relevant information and without losing accuracy on the results.

The RB method is a powerful tool to solve parametrized equations. The idea is to project the solution on a small dimensional space, specific for our problem, instead of adopting a generic high-dimension approximating space, like the finite element space. The use of a model which is able to represent the problem with a small number of degrees of freedom, without losing accuracy, reduces heavily computational costs.

In this paper we adopt the RB method to approximate the solution of the parametrized equations governing the control problem. Control problems solved with the RB method were already faced by Ito and Ravindran [8], [6] and [7], however without considering multi-parametrized problems and adopting different solution procedures. Parameters can be sorted as control parameters (i.e depending, on control function), physical (like velocity field or diffusivity) and geometrical (i.e. related to different domain configurations). Geometrical parameters are particularly important in the optimal control framework, since they allow the solution of shape optimization problems. In our formulation we will foresee all three classes of parameters. Recently, Grepl [5] has proposed the solution of parabolic problems with reduced basis (also in the optimal control framework). Other applications of reduced basis methods are provided in the field of inverse problems with non-affine parametric dependence by Nguyen [10].

As a study case, we consider an air pollution control problem: our goal is to regulate the pollutant emission by industrial plants in order to keep pollution

below an acceptable level over an observation area, e.g. a town. We refer to air pollution phenomena in a stationary frame on urban scales.

In Section 2 we formulate a generic control problem, for a linear time-independent advection-diffusion equation. In Section 3 we describe the reduced basis approximation for the solution of the parametrized equations governing the control problem. In Section 4 we report some features of the air pollution control problem, then we apply the formulation presented in Section 2 to derive our model. In Sections 5, 6 and 7 we present the parametrized state and adjoint equations, some numerical results and an example for the case of control, physical and geometrical input, respectively. Some preliminary results were reported in [12]. In Section 8 we report some concluding remarks and indicate a perspective on further developments.

## 2 Optimal control problem for advection-diffusion equations

Let us consider an advection-diffusion problem defined on the domain  $\Omega \subset \mathbb{R}^2$ :

$$\begin{cases} Aw \equiv -\nabla \cdot (\nu \nabla w) + \mathbf{V} \cdot \nabla w = u \text{ in } \Omega, \\ w = 0 \text{ on } \Gamma_D, \\ \frac{\partial w}{\partial \mathbf{n}} = 0 \text{ on } \Gamma_N, \end{cases} \quad (1)$$

where  $w$  is the state variable,  $u$  the control function defined on the domain,  $\mathbf{V}$  the velocity field and  $\nu$  is the diffusivity that may depend on the domain coordinates  $(x, y)$ . A homogeneous Dirichlet condition is imposed on the inflow boundary  $\Gamma_D := \{\mathbf{x} \in \partial\Omega : \mathbf{V}(\mathbf{x}) \cdot \mathbf{n}(\mathbf{x}) < 0\}$ , where  $\mathbf{n}(\mathbf{x})$  is the unit vector directed outward, and a homogeneous Neumann condition on  $\Gamma_N := \partial\Omega \setminus \Gamma_D$ . Defining  $H_{\Gamma_D}^1 := \{v \in H^1(\Omega) : v|_{\Gamma_D} = 0\}$ , the weak form of the state equation (1) is: *find*  $w \in H_{\Gamma_D}^1 : a(w, \varphi) = F(\varphi; u), \forall \varphi \in H_{\Gamma_D}^1$ , where

$$a(w, \varphi) := \int_{\Omega} \nu \nabla w \cdot \nabla \varphi \, d\Omega + \int_{\Omega} \mathbf{V} \cdot \nabla w \, \varphi \, d\Omega, \quad (2)$$

$$F(\varphi; u) := \int_{\Omega} u \varphi \, d\Omega. \quad (3)$$

We then define the observation of the system on a part  $D \subset \Omega$  of the domain through the cost functional:  $J(u, w) = \frac{1}{2} \int_D (w(u) - z_d)^2 dD$ , where  $z_d$  is the desired observation.

The Lagrangian functional reads:  $\mathcal{L}(w, p, u) = J(u) + F(p; u) - a(w, p)$ , where  $w, p \in H_{\Gamma_D}^1(\Omega)$  and  $u \in L^2(\Omega)$ . By differentiating  $\mathcal{L}$  with respect to the state variable, we obtain the weak form for the adjoint equation: *find*  $p \in H_{\Gamma_D}^1 : a^{ad}(p, \phi) = F^{ad}(\phi; w), \forall \phi \in H_{\Gamma_D}^1$ , where

$$a^{ad}(p, \phi) := \int_{\Omega} \nu \nabla p \cdot \nabla \phi \, d\Omega + \int_{\Omega} \mathbf{V} \cdot \nabla \phi \, p \, d\Omega, \quad (4)$$

$$F^{ad}(\phi, w) := \int_{\Omega} (w - z_d) \phi \, dD, \quad (5)$$

whose differential form is:

$$\begin{cases} A^*p \equiv -\nabla \cdot (\nu \nabla p + \mathbf{V} \cdot p) = \chi_D(w - z_d) \text{ in } \Omega, \\ p = 0 \text{ on } \Gamma_D, \\ \nu \frac{\partial p}{\partial n} + \mathbf{V} \cdot \mathbf{n}p = 0 \text{ on } \Gamma_N, \end{cases} \quad (6)$$

where  $\chi_D$  is the characteristic function of the subdomain  $D$ .

By differentiating the Lagrangian functional with respect to the control function  $u$ , we obtain the weak form of the optimal control constraint:  $\langle J'(u), \psi \rangle = \int_{\Omega} p \psi \, d\Omega = 0, \quad \forall \psi \in L^2(\Omega)$ .

We solve our problem using an iterative method where the variation of control function is led by a gradient method. From the optimal control constraint, we can derive a stopping criterium for the iterative method. At the  $k^{th}$  step of the iterative method:

- we solve the state equation:  
find  $w^k \in \mathbf{H}_{\Gamma_D}^1$  :  $a(w^k, \varphi) = F(\varphi; u^k), \quad \forall \varphi \in \mathbf{H}_{\Gamma_D}^1$ ;
- we solve the adjoint equation:  
find  $p^k \in \mathbf{H}_{\Gamma_D}^1$  :  $a^{ad}(p^k, \phi) = F^{ad}(\phi; w^k), \quad \forall \phi \in \mathbf{H}_{\Gamma_D}^1$ ;
- if the stopping criterium is not satisfied, we update the control function

$$u^{k+1} = u^k + \delta u^k \quad \delta u^k = -\tau^k J'(u^k) = -\tau^k p^k. \quad (7)$$

The stopping criterium adopted is [3]:

$$\|p^k\|_{L^2} < tol, \quad (8)$$

to check if our adjoint variable  $p^k$  is too small to produce a significative variation  $\delta u^k$  on the new control function  $u^{k+1}$ .

## 2.1 Numerical discretization and stabilization

Both state and adjoint equations are advection-diffusion equations; since the transport term dominates the diffusion one [4], a suitable numerical stabilization is needed. We adopt the *stabilized Lagrangian* [3],[2], instead of stabilizing separately state and adjoint equations in a conventional manner [13]. In this way, stabilization is not only based on a strongly consistent method, but also there is coherence between state and adjoint stabilized equations.

In this work we have adopted the approach “optimize-then-discretize” to solve optimal control problems, we have formulated an optimality condition, from this condition we have built an adjoint problem and then we discretize both state and adjoint equations. An alternative approach would be “discretize then optimize”

which has been considered for the same kind of problem in [12]. Indicating with the index  $h$  the discretized quantities, the stabilized state equation reads:

$$\text{find } w_h \in X_h : a_h(w_h, \varphi_h) = F_h(\varphi_h; u_h), \quad \forall \varphi_h \in X_h, \quad (9)$$

with:

$$a_h(w_h, \varphi_h) := a(w_h, \varphi_h) - \sum_{K \in \mathcal{T}_h} \delta_K \int_K Aw_h A^* \varphi_h dK,$$

$$F_h(\varphi_h; u_h) := F(\varphi_h; u_h) - \sum_{K \in \mathcal{T}_h} \delta_K \int_K u_h A^* \varphi_h dK,$$

where  $A$  is the state operator and  $A^*$  is the adjoint operator. The terms  $a(w_h, \varphi_h)$  and  $F(\varphi_h; u_h)$  are defined in (2), (3),  $w_h$  and  $u_h$  are discrete approximations of the functions  $w$ ,  $u$ , and  $X_h \subset H_{\Gamma_D}^1$  is the finite element space built up on a grid  $\mathcal{T}_h$ , so that the computational domain is  $\bar{\Omega} = \bigcup_{K \in \mathcal{T}_h} K$  (see [13]).

The adjoint equation is:

$$\text{find } p_h \in X_h : a_h^{ad}(p_h, \phi_h) = F_h^{ad}(\phi_h; w_h; u_h), \quad \forall \phi_h \in X_h, \quad (10)$$

where:

$$a_h^{ad}(p_h, \phi_h) := a^{ad}(p_h, \phi_h) - \sum_{K \in \mathcal{T}_h} \delta_K \int_K A^* p_h A \phi_h dK,$$

$$F_h^{ad}(\phi_h; w_h; u_h) := F^{ad}(\phi_h; w_h) - \sum_{K \in \mathcal{T}_h} \delta_K \int_K \left( \chi_D (w_h - z_d) \cdot \right.$$

$$\left. A \phi_h + (Aw_h - u_h) \chi_D \phi_h \right) dK.$$

Note that the terms  $a^{ad}(p_h, \phi_h)$  and  $F^{ad}(\phi_h; w_h)$  are defined in (4) and (5) and  $p_h$  is the discrete approximation of the function  $p$ .

### 3 Reduced basis method for optimal control

As anticipated in the Introduction, we consider three different types of input parameters: control input  $\mu_u$ , which parametrizes the control function  $u = u(\mu_u)$ ; physical input  $\mu_p$ , like, for ex., velocity field  $\mathbf{V}$  and viscosity  $\nu$ ; geometrical input  $\mu_g$ , which characterizes the domain geometry. These parameter classes allow us to solve different types of control problems. Of course, inputs can be combined together to form, for example, a control-physical input (i.e. control and physical quantities as parameters). In this section, for convenience, we refer to a generic input  $\boldsymbol{\mu} = \{\mu_u, \mu_p, \mu_g\}$ , without specifying its own nature.

We introduce a set of parameter samples  $S_N = \{\boldsymbol{\mu}^1, \dots, \boldsymbol{\mu}^N\}$ , where  $\boldsymbol{\mu}^n \in \mathcal{D}$ ,  $n = 1, \dots, N$ . For each input vector in  $S_N$ , we calculate a finite element method

solution of the state equation  $w_h(\boldsymbol{\mu}^n)$  in the space  $X_h$ ; we choose a discretization refined enough to ensure that the solution in the high-dimensional space  $X_h$  is accurate enough to approximate the exact solution in  $H_{\Gamma_D}^1$ . We do the same for the adjoint problem: we select a set of  $N$  samples  $S_N^{ad} = \{\boldsymbol{\mu}_{ad}^1, \dots, \boldsymbol{\mu}_{ad}^N\}$ , where  $\boldsymbol{\mu}_{ad}^n \in \mathcal{D}$ ,  $n = 1, \dots, N$ , and correspondingly we compute the finite element approximation of the adjoint variable  $p_h(\boldsymbol{\mu}_{ad}^n) \in X_h$ . The two sets  $S_N$  and  $S_N^{ad}$  are chosen independently. Also the reduced basis formulation and the basis construction procedure have been influenced by the choice of using the approach “optimize-then-discretize” for the optimal control problem. We then introduce the reduced basis spaces:

$$W_N = \text{span}\{\zeta^n \equiv w_h(\boldsymbol{\mu}^n), n = 1, \dots, N\} \quad (11)$$

for the state problem and

$$Z_N = \text{span}\{\xi^n \equiv p_h(\boldsymbol{\mu}_{ad}^n), n = 1, \dots, N\} \quad (12)$$

for the adjoint problem. According to (11) and (12),  $W_N$  and  $Z_N$  consist of all functions in  $X_h$  that can be expressed as a linear combination of, respectively,  $\zeta^n$  and  $\xi^n$ . We assume linear independence of the basis functions.

Starting from the state variable, in the RB approach we look for an approximation  $w_N(\boldsymbol{\mu})$  in  $W_N$ , that can be regarded as a *surrogate* of the finite element approximation  $w_h(\boldsymbol{\mu})$ ; we can express the RB solution  $w_N(\boldsymbol{\mu})$  as:

$$w_N(\boldsymbol{\mu}) = \sum_{j=1}^N w_{N_j}(\boldsymbol{\mu}) \zeta^j = (\underline{w}_N(\boldsymbol{\mu}))^T \underline{\zeta}, \quad (13)$$

where  $\underline{w}_N(\boldsymbol{\mu}) \in \mathbb{R}^N$  is the column vector of the linear combination coefficient  $w_{N_j}$ ,  $j = 1, \dots, N$ .

Let  $p_N$  be the RB approximation of the adjoint variable:

$$p_N(\boldsymbol{\mu}) = \sum_{j=1}^N p_{N_j}(\boldsymbol{\mu}) \xi^j = (\underline{p}_N(\boldsymbol{\mu}))^T \underline{\xi}. \quad (14)$$

The underlying idea of the RB method is a projection onto a lower-order approximation space, specific for the problem of interest, instead of a general high-order one. The conjecture is that we should be able to accurately represent the solution corresponding to some new points in parameter space,  $\boldsymbol{\mu}^{new}$ , as an appropriate combination of solutions previously computed at a small number of sample points in parameter space ( $\boldsymbol{\mu}^n$  and  $\boldsymbol{\mu}_{ad}^n$ ,  $n = 1, \dots, N$ ). In this case we are interested in solving the optimal control problem and finding the control function by evaluating the cost functional in a rapid, reliable and repeated way. At each iterative step of the method adopted to solve the control problem, for any given  $\boldsymbol{\mu} \in \mathcal{D}$  and the corresponding control function  $u$  (7), we compute the reduced basis approximation of the state variable  $w_N(\boldsymbol{\mu}) \in W_N$ , by solving

$$a(w_N(\boldsymbol{\mu}), v; \boldsymbol{\mu}) = F(v; u), \quad \forall v \in W_N.$$

Once  $w_N$  is available, we determine the solution  $p_N \in Z_N$  of the adjoint equation:

$$a^{ad}(p_N(\boldsymbol{\mu}), \phi; \boldsymbol{\mu}) = F^{ad}(\phi, w_N(\boldsymbol{\mu})), \quad \forall \phi \in Z_N.$$

Finally we evaluate the reduced basis approximation of our output, i.e. the cost function  $J(u, w_N)$  and the adjoint variable  $p_N$ , then we check whether the stopping criterium is satisfied.

To apply the reduced basis method, we shall suppose that for some finite (preferably small) integers  $Q$  and  $Q^{ad}$ , the bilinear forms  $a(\cdot, \cdot; \boldsymbol{\mu})$  and  $a^{ad}(\cdot, \cdot; \boldsymbol{\mu})$  can be expressed as follows:

$$a(w, v; \boldsymbol{\mu}) = \sum_{q=1}^Q \sigma^q(\boldsymbol{\mu}) a^q(w, v), \quad \forall w, v \in \mathbf{H}_{\Gamma_D}^1, \quad \forall \boldsymbol{\mu} \in \mathcal{D},$$

$$a^{ad}(p, \phi; \boldsymbol{\mu}) = \sum_{q=1}^{Q^{ad}} \sigma_{ad}^q(\boldsymbol{\mu}) a_{ad}^q(p, \phi), \quad \forall p, \phi \in \mathbf{H}_{\Gamma_D}^1, \quad \forall \boldsymbol{\mu} \in \mathcal{D},$$

for some suitable  $\sigma^q(\boldsymbol{\mu}) : \mathcal{D} \rightarrow \mathbb{R}$ ,  $a^q : \mathbf{H}_{\Gamma_D}^1 \times \mathbf{H}_{\Gamma_D}^1 \rightarrow \mathbb{R}$ ,  $q = 1, \dots, Q$ , and for some  $\sigma_{ad}^q(\boldsymbol{\mu}) : \mathcal{D} \rightarrow \mathbb{R}$ ,  $a_{ad}^q : \mathbf{H}_{\Gamma_D}^1 \times \mathbf{H}_{\Gamma_D}^1 \rightarrow \mathbb{R}$ ,  $q = 1, \dots, Q^{ad}$ . This is an assumption of affine parameter dependence and is crucial to computational efficiency because it allows to split the computing procedure. We assume also affine parameter dependence for the functionals  $F$  and  $F^{ad}$ .

Coming to the matrix form, we define the matrices  $\underline{A}_N(\boldsymbol{\mu}) = a(\zeta^i, \zeta^j; \boldsymbol{\mu})$  and  $\underline{A}_N^{ad}(\boldsymbol{\mu}) = a^{ad}(\xi^i, \xi^j; \boldsymbol{\mu})$ ,  $1 \leq i, j \leq N$ , and the vectors  $\underline{F}_N = F(\zeta^j, u)$  and  $\underline{F}_N^{ad} = F^{ad}(\xi^j, w_N)$ ,  $1 \leq j \leq N$ . It is a simple matter to observe that:

$$\underline{A}_N(\boldsymbol{\mu}) = \sum_{q=1}^Q \sigma^q(\boldsymbol{\mu}) \underline{A}^q, \quad \underline{A}_N^{ad}(\boldsymbol{\mu}) = \sum_{q=1}^{Q^{ad}} \sigma_{ad}^q(\boldsymbol{\mu}) \underline{A}_{ad}^q, \quad (15)$$

where  $A_{i,j}^q = a^q(\zeta^i, \zeta^j)$ ,  $1 \leq i, j \leq N$ ,  $1 \leq q \leq Q$ , and  $A_{ad,i,j}^q = a_{ad}^q(\xi^i, \xi^j)$ ,  $1 \leq i, j \leq N$ ,  $1 \leq q \leq Q^{ad}$ . Note that  $\underline{A}^q \in \mathbb{R}^{N \times N}$ ,  $1 \leq q \leq Q$ , and  $\underline{A}_{ad}^q$ ,  $1 \leq q \leq Q^{ad}$ , are *independent* of the input parameter  $\boldsymbol{\mu}$ .

We can then reformulate the state equation as: given  $\boldsymbol{\mu} \in \mathcal{D}$ , find the unique solution  $\underline{w}_N(\boldsymbol{\mu})$  to

$$\underline{A}_N(\boldsymbol{\mu}) \underline{w}_N(\boldsymbol{\mu}) = \underline{F}_N, \quad (16)$$

and the adjoint equation as: given  $\boldsymbol{\mu} \in \mathcal{D}$  and  $\underline{w}_N(\boldsymbol{\mu})$ , find the unique solution  $\underline{p}_N(\boldsymbol{\mu})$  to

$$\underline{A}_N^{ad}(\boldsymbol{\mu}) \underline{p}_N(\boldsymbol{\mu}) = \underline{F}_N^{ad}. \quad (17)$$

### 3.1 Computational procedure: off-line/on-line decomposition

Since the matrices  $\underline{A}^q$  and  $\underline{A}_{ad}^q$  are parameter-independent, they can be computed only once and for all.

Indeed, in an *off-line* stage, we find  $\zeta^i, \xi^i, i = 1, \dots, N$ , and form  $\underline{A}^q$ , for  $1 \leq q \leq Q$ ,  $\underline{A}_{ad}^q$ , for  $1 \leq q \leq Q^{ad}$ , and  $\underline{F}_N, \underline{F}_N^{ad}$ . Then in an *on-line* stage, for any given new  $\boldsymbol{\mu}$ , we only need to form  $\underline{A}_N(\boldsymbol{\mu})$  from the  $\underline{A}^q$ ,  $\underline{A}_N^{ad}(\boldsymbol{\mu})$  from the  $\underline{A}_{ad}^q$ , through (15), then solve (16) for  $\underline{w}_N(\boldsymbol{\mu})$  and (17) for  $\underline{p}_N(\boldsymbol{\mu})$  and finally evaluate  $J(u, w_N; \boldsymbol{\mu})$ . For an analysis of the computational costs of the two stages, see [11].

Note that the two processes are completely decoupled. The expensive off-line computation can be processed at an early stage and needs to be done only once. The efficient on-line computation can then be used for very fast evaluations of outputs at different points in the parameter space. The incremental cost to evaluate the output for any given new  $\boldsymbol{\mu}$  is very small: first because  $N$  is very small (typically of the order of 10, owing to the good convergence properties of  $W_N$  and  $Z_N$  [11]); and second because (16) and (17) can be inverted very rapidly.

### 3.2 Error on control and error on cost functional

When solving a simple equation, for example the state equation, by the reduced basis approach we look for an approximation  $w^N(\boldsymbol{\mu})$  (to  $w_h(\boldsymbol{\mu})$ ) in  $W_N$ . In fact  $w^N$  is expressed by a linear combination of FE functions computed on a grid  $\mathcal{T}_h$ . Thus we should indicate it as  $w_h^N$ , however the subindex  $h$  will be omitted for simplicity of notation. As a preliminary test we are interested to check that the control problem solved with the finite element method and the one solved with the reduced basis method (when the basis functions are calculated on the same mesh) converge to the same control solution, although they evolve separately. To this aim, we define

$$\varepsilon_u = \int_{\Omega} (u_h^f - u_N^f)^2 d\Omega; \quad \varepsilon_J = |J^f(u_N, w_N) - J^f(u_h, w_h)|,$$

i.e. the square of the  $L^2$ -norm of the difference on the control and the error on the cost functional evaluation, respectively, at convergence of the optimization process. Here  $f$  stands for *final* and refers to values taken at convergence, while  $u_h^f$  and  $u_N^f$  are given by:

$$u_h^f = u_h^{f-1} - \tau J'(u_h^{f-1}) = u_0 - \tau \sum_{i=1}^{f-1} J'(u_h^i), \quad u_N^f = u_N^{f-1} - \tau J'(u_N^{f-1}) = u_0 - \tau \sum_{i=1}^{f-1} J'(u_N^i),$$

where  $u_0$  is the initial control function for both iterative processes.

We note that:

$$\varepsilon_u = \int_{\Omega} \left( \tau \sum_{i=1}^{f-1} \left( J'(u_N^i) - J'(u_h^i) \right) \right)^2 d\Omega = \tau^2 \sum_{i=1}^{f-1} \int_{\Omega} \left( p_N^i - p_h^i \right)^2 d\Omega,$$

since  $J' = p$  by Riesz theorem: thus  $\varepsilon_u$  at convergence depends on the sum, extended to all previous iterations, of the errors on the adjoint variable, multiplied



by the relaxation parameter  $\tau > 0$ . So the larger number of iterations to converge, the larger  $\varepsilon_u$ . We want that even in the worst case, where many iterations are necessary before converging  $\varepsilon_u$ , be still small. Further we use an adaptive procedure for the construction of the basis (see [14]), so that the dimension of the reduced basis space  $N$  is large enough to ensure that the errors  $\varepsilon_u$  and  $\varepsilon_J$  are “small” in any case.

## 4 Application: control of air pollution

Now we consider a particular case of control problem governed by an advection diffusion equation: our goal is to regulate the pollutant emission (in large part Sulfur Dioxide) by industrial plants in order to keep the pollutant level below a fixed threshold over an observation area, for instance a town. This application can be regarded as an extension of the one presented in [3] and [12], in which we account for parametric dependence of our equations. We refer to the do-

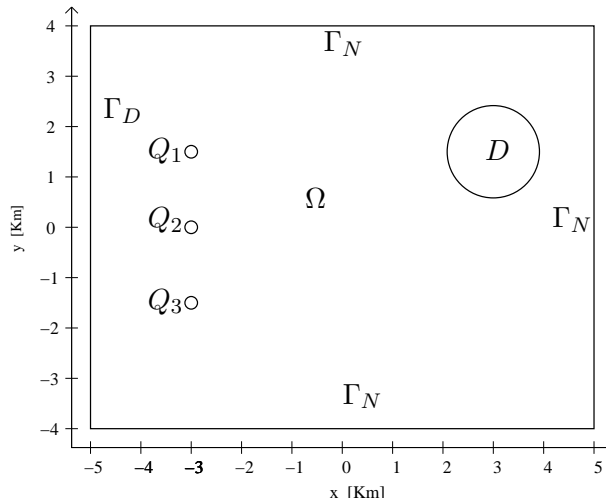


Figure 1: Reference domain for pollution control problem

main in Fig.1: the scale is urban (the dimension of the domain is in the range  $10 - 50 \text{ Km}$ ),  $Q_1$ ,  $Q_2$ ,  $Q_3$  are the three chimneys emitting pollutant and  $D$  is the observation area. Admitted pollutants concentrations are ruled by normative, changing from Country to Country. Typically there are two limits: *attention level* and *alarm level*.

Our purpose is to develop a systematical method to control, for example,  $\text{SO}_2$  emission so that pollution concentration over a certain area  $D$  is acceptable (i.e., below attention level), taking into account wind and meteorological conditions in a stationary frame.

We consider three different *atmospherical stability classes* [4]: *stable atmosphere* - air vertical motions are slowed down so that vertical diffusion is poor; *neutral atmosphere* - indifferent equilibrium to air vertical motion so that vertical diffusion is mostly due to mechanical turbulence; *unstable atmosphere* - pollutant diffusion is enhanced.

We adopt a 2D transport-diffusion equation to govern pollutant concentration at effective height (chimney's geometrical height + smokes raising height) and we project this concentration down to the ground by analogy with the Gauss model [4].

For our simulations, we take  $110 \mu\text{g}/\text{m}^3$  as target concentration level  $z_d$  and  $H = 100 \text{ m}$  as the effective height.

#### 4.1 The mathematical model for the air pollution problem

Pollutant concentration distribution at effective height satisfies the state equation (1), where  $\nu$  represents the turbulent diffusivity term, instead of the usual molecular diffusivity, thus  $\mathbf{V}$  describes the mean motion of the air, rather than the wind velocity field [3]. Diffusivity  $\nu$  depends on problem type, domain geometry and atmospheric conditions. In Fig.2  $\nu$  is reported as function of the  $x$  coordinate for each stability class. We assume  $u = \sum_{i=1}^3 u_i \chi_{Q_i}$ , being  $\chi_{Q_i}$  the characteristic function of the region occupied by the chimney  $Q_i$  and  $u_i$  the rate of pollutant issuing from the  $i$ -th source. Then Eq.(3) can be written as:  $F(\varphi; u) = \sum_{i=1}^3 \int_{Q_i} u_i \varphi \, dQ_i$ . When solving the control problem with the iter-

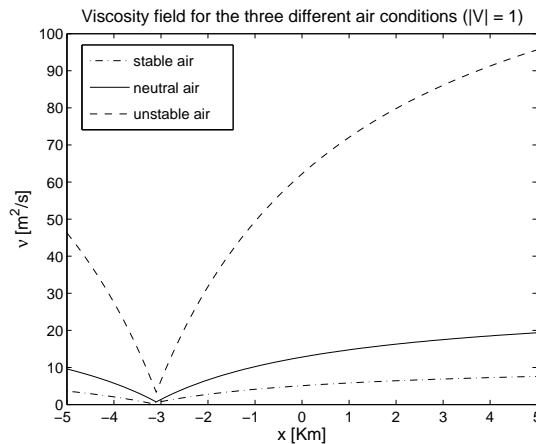


Figure 2: Viscosity as function of the  $x$  coordinate for the three stability classes.

ative method, at each step we update the control function with the following increment:  $\delta u^k = \sum_{i=1}^3 \delta u_i^k = -\tau \sum_{i=1}^3 p \chi_{Q_i}$ .

In analogy with the Gauss model [4], which is a simple tool to predict concentration at a given height of a pollutant emitted by a chimney, we introduce

a projection term of pollutant concentration at ground:  $g(x, y) = 2e^{-\frac{1}{2}(\frac{H}{\sigma_z})^2}$ , where  $\sigma_z$  is a model dispersion coefficient which accounts for meteorological stability class and soil orography. Values typically considered for urban soil are [3]:  $\sigma_z = 0.012x(1 + 0.0002x)^{-\frac{1}{2}}$  [m] for stable air;  $\sigma_z = 0.040x(1 + 0.0002x)^{-\frac{1}{2}}$  [m] for neutral air;  $\sigma_z = 0.220x(1 + 0.0001x)^{-\frac{1}{2}}$  [m] for unstable air.

## 5 Control input: variable emission rates

We consider a two components control input parameter  $\boldsymbol{\mu}_u = \{u_1, u_2\}$ . We fix a total emission value  $u_{tot} = 2700$  g/s corresponding to the industrial plant working at its maximum productivity and write  $u_3 = 2700 - u_1 - u_2$  and  $\boldsymbol{\mu}_u \in \mathcal{D}$ , where  $\mathcal{D} = [0, 2700] \times [0, 2700]$  with  $u_1 + u_2 \leq 2700$ .

### 5.1 Parametrized state equation

The residuals of equations (1) and (6) are:

$$R(w_h, u_h) := Aw_h - u_h, \quad R^{ad}(p_h, w_h) := A^*p_h - L(w_h)$$

where  $L(w_h) := \chi_{Dg}(g w_h - z_d)$ . To compute the reduced basis approximation of the state variable (13), we need to find the  $N$  unknown components  $w_{N_j}(\boldsymbol{\mu}_u)$  by solving the system:

$$a_h(w_N(\boldsymbol{\mu}_u), \zeta_i) = F_h(\zeta_i) \quad i = 1, \dots, N, \quad (18)$$

where

$$a_h(w_N(\boldsymbol{\mu}_u), \zeta_i) = \sum_{j=1}^N w_{N_j}(\boldsymbol{\mu}_u) \left[ \sum_{K \in \mathcal{T}_h} \int_K \nu \nabla \zeta_j \cdot \nabla \zeta_i + \sum_{K \in \mathcal{T}_h} \int_K (\mathbf{V} \cdot \nabla \zeta_j) \zeta_i - \sum_{K \in \mathcal{T}_h} \delta_K \int_K A \zeta_j A^* \zeta_i \right] \quad (19)$$

and

$$F_h(\zeta_i) = \sum_{K \in \mathcal{T}_h} \int_K u_h(\boldsymbol{\mu}_u) \zeta_i - \sum_{K \in \mathcal{T}_h} \delta_K \int_K u_h(\boldsymbol{\mu}_u) A^* \zeta_i. \quad (20)$$

We define now the following matrices, related to the diffusive, convective and stabilization terms, respectively:

$$C_{i,j} = \sum_{K \in \mathcal{T}_h} \int_K \nu \nabla \zeta_j \cdot \nabla \zeta_i, \quad (21)$$

$$B_{i,j} = \sum_{K \in \mathcal{T}_h} \int_K (\mathbf{V} \cdot \nabla \zeta_j) \zeta_i, \quad (22)$$

$$S_{i,j} = - \sum_{K \in \mathcal{T}_h} \delta_K \int_K A \zeta_j A^* \zeta_i. \quad (23)$$

The matrix  $\underline{A}_N$  (15) can thus be written as:  $\underline{A}_N = \underline{C} + \underline{B} + \underline{S}$ .  
 In this particular case,  $\underline{A}_N$  is independent of the input parameter  $\boldsymbol{\mu}_u$ .  
 Let us define also the following column vectors depending on  $\boldsymbol{\mu}_u$ :

$$G_i(\boldsymbol{\mu}_u) = \sum_{K \in \mathcal{T}_h} \int_K u_h(\boldsymbol{\mu}_u) \zeta_i, \quad (24)$$

$$H_i(\boldsymbol{\mu}_u) = - \sum_{K \in \mathcal{T}_h} \delta_K \int_K u_h(\boldsymbol{\mu}_u) A^* \zeta_i, \quad (25)$$

so that  $\underline{F}_N(\boldsymbol{\mu}_u) = \underline{G}(\boldsymbol{\mu}_u) + \underline{H}(\boldsymbol{\mu}_u)$ . The unknown vector  $\underline{w}_N(\boldsymbol{\mu}_u)$  is the solution of the system:

$$\underline{A}_N \underline{w}_N(\boldsymbol{\mu}_u) = \underline{F}_N(\boldsymbol{\mu}_u). \quad (26)$$

## 5.2 Parametrized adjoint equation

The  $N$  unknown components  $p_{N_j}(\boldsymbol{\mu}_u)$  for the reduced basis approximation of adjoint variable (14) are the solution of the problem:

$$a_h^{ad}(p_N(\boldsymbol{\mu}_u), \xi_i) = F_h^{ad}(\xi_i; w_N, u_h) \quad i = 1, \dots, N, \quad (27)$$

where

$$a_h^{ad}(p_N(\boldsymbol{\mu}_u), \xi_i) = \sum_{j=1}^N p_{N_j}(\boldsymbol{\mu}_u) \left[ \sum_{K \in \mathcal{T}_i} \int_K \nu \nabla \xi_j \cdot \nabla \xi_i + \sum_{K \in \mathcal{T}_h} \int_K (\mathbf{v} \cdot \nabla \xi_i) \xi_j - \sum_{K \in \mathcal{T}_h} \delta_K \int_K A^* \xi_j A \xi_i \right], \quad (28)$$

and

$$F_h^{ad}(\xi_i; w_N(\boldsymbol{\mu}_u), u_h) = \sum_{K \in \mathcal{T}_h} \int_K \chi_{DG}(g w_N(\boldsymbol{\mu}_u) - z_d) \xi_i - \quad (29)$$

$$\sum_{K \in \mathcal{T}_h} \delta_K \int_K L(w_N(\boldsymbol{\mu}_u)) A \xi_i - \sum_{K \in \mathcal{T}_h} \delta_K \int_K R(w_N(\boldsymbol{\mu}_u), u_h) L'(\xi_i).$$

We now define  $\underline{B}^{ad}$ ,  $\underline{S}^{ad}$  through their components:

$$B_{i,j}^{ad} = \sum_{K \in \mathcal{T}_h} \int_K (\mathbf{v} \cdot \nabla \xi_i) \xi_j = B_{j,i}, \quad (30)$$

$$S_{i,j}^{ad} = - \sum_{K \in \mathcal{T}_h} \delta_K \int_K A^* \xi_j A \xi_i = S_{j,i}, \quad (31)$$

where  $B_{j,i}$ ,  $S_{j,i}$  are defined by (22), (23). Then matrix  $\underline{A}_N^{ad} = \underline{C} + \underline{B}^{ad} + \underline{S}^{ad}$ . Let  $\underline{G}^{ad}$ ,  $\underline{H}^{ad}$ ,  $\underline{I}^{ad}$  be the column vectors defined as:

$$G_i^{ad} = \sum_{K \in \mathcal{T}_h} \int_K \chi_D g \xi_i, \quad (32)$$

$$H_i^{ad} = - \sum_{K \in \mathcal{T}_h} \delta_K \int_K \chi_D g \xi_i A \xi_i, \quad (33)$$

$$I_i^{ad} = - \sum_{K \in \mathcal{T}_h} \delta_K \int_K \chi_D g^2 \xi_i (A \xi_i - u_h). \quad (34)$$

All the matrices  $\underline{C}$ ,  $\underline{B}^{ad}$ ,  $\underline{S}^{ad}$  and the vectors  $\underline{G}^{ad}$ ,  $\underline{H}^{ad}$ ,  $\underline{I}^{ad}$  are computed off-line (i.e only once and stored), while for every new  $\boldsymbol{\mu}_u$  we assemble on-line the right-hand-side  $\underline{F}_N^{ad}$ . The unknown vector  $\underline{p}_N(\boldsymbol{\mu}_p)$  is the solution of the system:

$$\underline{A}_N^{ad} \underline{p}_N(\boldsymbol{\mu}_u) = \underline{F}_N^{ad}(\boldsymbol{\mu}_u). \quad (35)$$

### 5.3 Some results and one example

In Tab.1 we report the number of basis functions (for both state and adjoint equations), the mean error on cost functional and on control function at convergence (computed on a high number of random inputs) and the computational saving for neutral and unstable air. The convergence tolerance is  $tol = 10^{-7}$ . In the case of stable air, there is no need of finding an optimal solution, since pollutant concentration is always under attention level. The computational saving compares the time needed to perform the on-line steps with the one necessary to complete a finite element simulation using a mesh with about  $10^4$  elements. The number of basis functions and the saving percentages are the same for the two cases. The orders of magnitude of the errors are nearly the same.

In Tab.2 we report some details regarding only the state equation: the mean  $H^1$ -error with respect to the finite element solution (computed on a high number of random inputs) and the computational saving for the three different air conditions. The number of basis functions for the reduced basis approximation of state problem is  $N = 7$  for the three cases. Dealing with a test case we calculated several errors on control function, on cost functional and its gradient. To show an example, we start from the upper chimney emitting at 45% of  $u_{tot}$  and the central switched off, that is  $\boldsymbol{\mu}_u = \{1215, 0\}$  [g/s], in neutral air. The control problem solved with the two methods (finite element and reduced basis) leads for both to the following optimal solution: the upper chimney emission rate is reduced to 3.49%, central chimney remains switched off and the lower one work at 55.02% of  $u_{tot}$ . Fig.3 shows the reduced basis approximations of both initial and optimal solutions.

Table 1: Control input: number of basis functions, mean errors on cost functional and on control function at convergence and time saving for neutral and unstable air.

Air condition	$N$	Mean error on J	Mean $H^1$ -error on u	Saving
neutral	7	$1.4E - 11$	$2.5E - 5$	90%
unstable	7	$1.9E - 12$	$6.1E - 6$	90%

Table 2: Control input for state equation: mean  $H^1$ -error and time saving for the three air conditions.

Air condition	mean $H^1$ -error	Saving
stable	$1E - 8$	96%
neutral	$2.1E - 8$	94%
unstable	$3.7E - 8$	90%

## 6 Physical input: variable emission rates and wind direction

This case is more complex: we consider an input made of four components  $\boldsymbol{\mu}_p = \{u_1, u_2, V_x, V_y\}$ . Once again  $u_3 = 2700 - u_1 - u_2$  g/s, having imposed  $u_1 + u_2 \leq u_{tot}$ , and we fix the velocity absolute value  $|\mathbf{V}| = 1$ . We assume that the wind velocity direction can vary in the interval  $[-40^\circ, 90^\circ]$ .

Noting that diffusivity can be written as  $\nu = \bar{\nu} \cdot n(x)$ , where  $\bar{\nu}$  is the diffusivity coefficient (with  $\bar{\nu} = 1/2$  for the case of control input). As physical input one could also choose the “diffusivity coefficient”. The coefficient  $\bar{\nu}$  is an air stability index: the smaller  $\bar{\nu}$ , the more stable the air. Since we already consider three atmospherical stability classes, it is more significant to take wind velocity direction as physical input.

### 6.1 Parametrized state equation

The  $N$  unknowns  $w_{N_j}(\boldsymbol{\mu}_p)$  (13) are the solution of the problem (18), where  $a_h$  and  $F_h$  respectively defined in (19) and (20).

The matrix  $\underline{A}_N$  can be written as follows:

$$\underline{A}_N(\boldsymbol{\mu}_p) = \underline{C} + V_x \underline{B}_x + V_y \underline{B}_y + \underline{S}(\boldsymbol{\mu}_p), \quad (36)$$

where  $\underline{C}$  is the matrix (21),  $\underline{S}$  is defined by (23) and  $\underline{B}_x$  and  $\underline{B}_y$  are given by:

$$B_{x_{i,j}} = \sum_{K \in T_h} \int_K (\mathbf{U}_x \cdot \nabla \zeta_j) \zeta_i, \quad (37)$$

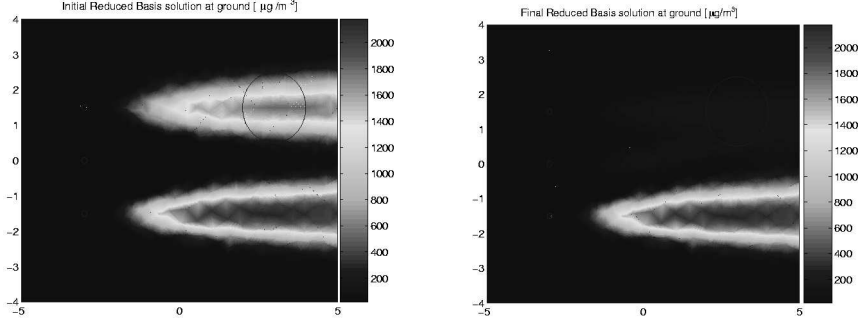


Figure 3: Control input: initial reduced basis solution (right) and final reduced basis solution (left) of state equation. Pollutant concentration is in  $[\mu g/m^3]$ .

$$B_{y_{i,j}} = \sum_{K \in T_h} \int_K (\mathbf{U}_y \cdot \nabla \zeta_j) \zeta_i, \quad (38)$$

with  $\mathbf{U}_x = (1, 0)$  and  $\mathbf{U}_y = (0, 1)$ ;  $\underline{B} = V_x \underline{B}_x + V_y \underline{B}_y$ , where  $\underline{B}$  (22) is the matrix related to the convective term.

The source term  $\underline{F}_N$  is given by:  $\underline{F}_N(\boldsymbol{\mu}_p) = \underline{G} + \underline{H}(\boldsymbol{\mu}_p)$ , where  $\underline{G}$  and  $\underline{H}$  are the vectors defined by (24) and (25).

All the parameter-independent matrices ( $\underline{C}$ ,  $\underline{B}_x$ ,  $\underline{B}_y$ ) are formed in the off-line stage, while matrices  $\underline{S}$ ,  $\underline{G}$ ,  $\underline{H}$ , depending on the parameter in a non-affine way, must be formed on-line for each new  $\boldsymbol{\mu}_p$ . Assembling of  $\underline{A}_N(\boldsymbol{\mu}_p)$  and  $\underline{F}_N(\boldsymbol{\mu}_p)$  is carried out in the on-line stage.

The unknown vector  $\underline{w}_N(\boldsymbol{\mu}_p)$  is the solution of the system:

$$\underline{A}_N(\boldsymbol{\mu}_p) \underline{w}_N(\boldsymbol{\mu}_p) = \underline{F}_N(\boldsymbol{\mu}_p). \quad (39)$$

The difference between (26) and (39) is that in the latter also  $\underline{A}_N$  depends on input parameter  $\boldsymbol{\mu}_p$ . To improve efficiency of the assembling procedure we may apply the decomposition of non-affine terms by the empirical interpolation method introduced in [1].

## 6.2 Parameterized adjoint equation

We want to find the weights of the linear combination (14), in order to have the reduced basis approximation of the adjoint variable, solution of (27). Bilinear form  $a_h^{ad}$  and functional  $F_h^{ad}$  are the same as in (28) and (29).

Let  $\underline{A}_N^{ad}$  be the matrix:  $\underline{A}_N^{ad}(\boldsymbol{\mu}_p) = \underline{C} + V_x \underline{B}_x^{ad} + V_y \underline{B}_y^{ad} + \underline{S}^{ad}(\boldsymbol{\mu}_p)$ , where  $\underline{C}$  is defined by (21),  $\underline{S}^{ad}$  is the stabilization matrix (31) (now parameter-dependent). The elements of matrices  $\underline{B}_x^{ad}$  and  $\underline{B}_y^{ad}$  are given by:

$$B_{x_{i,j}}^{ad} = \sum_{K \in T_h} \int_K (\mathbf{U}_x \cdot \nabla \xi_i) \xi_j = B_{x_{j,i}}, \quad B_{y_{i,j}}^{ad} = \sum_{K \in T_h} \int_K (\mathbf{U}_y \cdot \nabla \xi_i) \xi_j = B_{y_{j,i}},$$

with  $\mathbf{U}_x = (1, 0)$  and  $\mathbf{U}_y = (0, 1)$ , while  $B_{x_{j,i}}$  and  $B_{y_{j,i}}$  are (37) and (38). Moreover  $\underline{B}^{ad} = V_x \underline{B}_x^{ad} + V_y \underline{B}_y^{ad}$ , where  $\underline{B}^{ad}$  is the matrix related to the convective term (30).

The source term  $\underline{F}_N$  is given by:  $\underline{F}_N^{ad}(\boldsymbol{\mu}_p) = \underline{G}^{ad} + \underline{H}^{ad}(\boldsymbol{\mu}_p) + \underline{I}^{ad}(\boldsymbol{\mu}_p)$ . In this case,  $\underline{H}^{ad}$  (33) and  $\underline{I}^{ad}$  (34) are parameter-dependent, since they depend on velocity vector, while  $\underline{G}^{ad}$  (32) is parameter-independent. Also in this case an efficient computational procedure should be used.

The unknown vector  $\underline{p}_N(\boldsymbol{\mu}_p)$  is the solution of system:

$$\underline{A}_N^{ad}(\boldsymbol{\mu}_p) \underline{p}_N(\boldsymbol{\mu}_p) = \underline{F}_N^{ad}(\boldsymbol{\mu}_p). \quad (40)$$

Even in this case, the difference between (35) and (40) is that in the latter also  $\underline{A}_N^{ad}$  depends on input parameter  $\boldsymbol{\mu}_p$ .

### 6.3 Some results and one example

The use of the reduced basis method to solve both state and adjoint equations, at each step of our iterative method to solve control problem, implies several advantages from a computational point of view. In the case of control and physical input we have time savings up to 65-70%, which means that in the same time the finite element method solves just one iteration (state and adjoint equation using a mesh with about  $10^4$  elements), the reduced basis method solves 3 iterations. This is a good result dealing with optimal control problems, which are not real-time problems, but time savings could be even improved if we can adopt a stabilization method based on terms which can be built off-line. At present, stabilization is needed also in the reduced basis formulation because without using it, i.e. using the pure Galerkin method, we would find a “plateau” as  $N \rightarrow \infty$ , corresponding to the Galerkin residual evaluated for the stabilized “truth” solutions.

In our case, we can fix the velocity field (the desired online value) before applying optimal control (at first iteration) and so we can build  $S$  and  $S^{ad}$  offline or at a step we can call “pre-online” for our optimal control problem. Note that the basis has been assembled offline by considering different values for velocity field.

We report in Tab.3 the number of basis functions, the mean error on cost functional and on control function at convergence (computed on a high number of random inputs) and the computational saving (having fixed the “online” velocity field at first iteration) for neutral and unstable air, having imposed  $tol = 10^{-7}$ . Once again for stable air there is no need of searching an optimal solution, since the pollution level in town is always under attention level, whatever  $u_1$ ,  $u_2$  and  $u_3$  may be.

To understand the difference in the number of basis functions, we need to compare the weight of the diffusive term and the one of the convective term in  $\underline{A}_N$  (36). As diffusivity increases, diffusive term becomes dominant and so just “few”



Table 3: Physical input: number of basis functions, mean errors on cost functional and on control function at convergence and time saving for neutral and unstable air. Without fixing the online velocity field at first iteration the computational saving are  $\sim 65 - 70\%$ .

Air condition	$N$	Mean error on J	Mean $H^1$ -error on u	Saving
neutral	132	$0.9E - 9$	$2.5E - 7$	80%
unstable	81	$0.5E - 9$	$1.1E - 7$	80%

Table 4: Physical input for state equation: mean  $H^1$ -error and time saving for the three air conditions.

Air condition	mean $H^1$ -error	Saving
stable	$1.1E - 6$	95%
neutral	$3.8E - 7$	95%
unstable	$5.4E - 5$	90 - 95%

basis functions are needed to have a good approximation of the solution depending on convective velocity. Since for unstable air the diffusivity absolute value is higher, the convective term is less influent and fewer basis functions are needed. In Tab.4 we report some details on the state equation: the mean  $H^1$ -error with respect to the finite element solution (computed on a high number of random inputs) and the computational saving for the three different air conditions. The number of basis functions for the reduced basis approximation of state variable is  $N = 81$  for unstable air and  $N = 132$  for both neutral and stable air.

To show an example, we choose the following input:  $u_1 = 30\%$  and  $u_2 = 40\%$ , respectively, of  $u_{tot}$  and wind direction at  $45^\circ$  with respect to  $x$ -axis. Fig.4 shows the initial reduced basis solution and the reduced basis solution at convergence, with the upper chimney emitting at  $30.02\%$ , the central at  $38.81\%$  and the lower at  $7.27\%$ .

## 7 Geometrical input: parametrized domains

In this section we combine optimal control problems with geometrical sensitivity analysis. Our aim is twofold: to minimize pollutant concentration and maximize industrial production.

As an illustrative example we consider the physical domain  $\hat{\Omega} \subset \mathbb{R}^2$  at Fig.5, divided in seven subdomains  $\hat{\Omega}^r$ ,  $r = 1, \dots, 7$ . We have chosen the parameters  $\mu_g = \{C_1, C_2, C_3, C_4\}$ , with  $C_1 + C_2 = 3 \text{ Km}$  and  $C_3 + C_4 = 3 \text{ Km}$ . The central

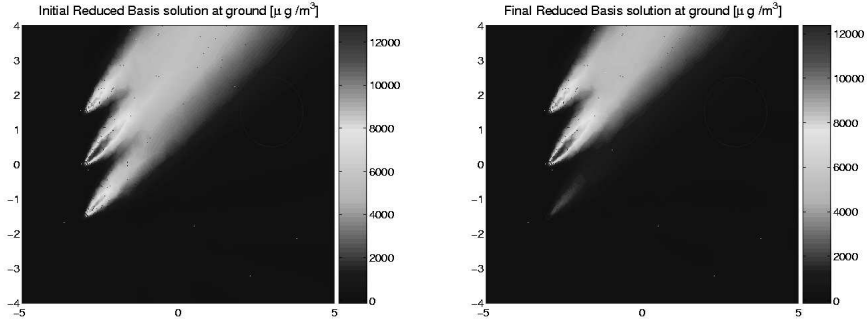


Figure 4: Physical input: initial reduced basis solution (right) and final reduced basis solution (left) of state equation. Pollutant concentration is in  $[\mu\text{g}/\text{m}^3]$ .

chimney position is fixed, while the position  $C_3$  of the upper chimney and the position  $C_2$  of the lower chimney can vary.

This kind of parametrized domain would allow, e.g., to answer the question on where to place a new chimney. The method is based on the affine mapping procedure from reference subdomains (the ones with  $C_1 = 2 \text{ Km}$ ,  $C_2 = 1 \text{ Km}$ ,  $C_3 = 1 \text{ Km}$  e  $C_4 = 2 \text{ Km}$ ) to the true ones ( $\Omega^r \rightarrow \hat{\Omega}^r$ ). This methodology can be extended to non-affine parametric dependence, see [1] and [15].

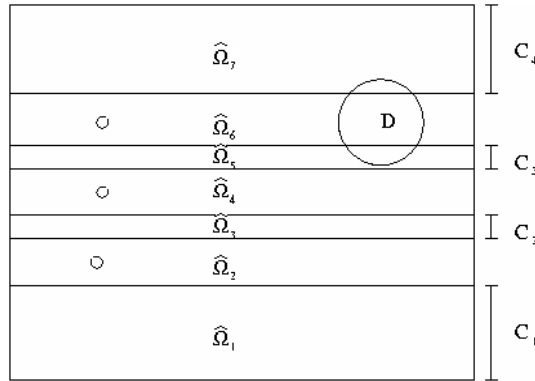


Figure 5: Scheme for the real computational domain: subdomains and parameters.

## 7.1 Parametrized state equation

Let  $R$  be the number of subdomains in which the real domain is divided:  $\hat{\Omega} = \bigcup_{r=1}^R \hat{\Omega}^r$ . We are interested in writing a partial differential equation depending on the set of geometrical parameters given as input. For this purpose, we refer the problem to a *reference domain* by an affine mapping from the “true”

subdomains  $\hat{\Omega}^r$  into the corresponding  $\Omega^r$ . For any  $\hat{x} \in \hat{\Omega}^r$ ,  $r = 1, \dots, R$ , its image  $x \in \Omega^r$  is given by:

$$x = \mathcal{G}^r(\boldsymbol{\mu}; \hat{x}) = G^r(\boldsymbol{\mu})\hat{x} + g^r, \quad 1 \leq r \leq R.$$

For convenience, we use  $\boldsymbol{\mu}$  instead of  $\boldsymbol{\mu}_g$ . After setting  $G_{ji}^r(\boldsymbol{\mu}) = \frac{\partial x_j}{\partial \hat{x}_i}$  on each subdomain  $r$  from the weak form of the state equation (9), we define the following bilinear and linear forms in the reference domain  $\Omega$ :

$$\mathcal{A}(w, v; \boldsymbol{\mu}) = \sum_{r=1}^R \int_{\Omega^r} \frac{\partial w}{\partial x_i} \left( G_{ii'}^r(\boldsymbol{\mu}) \hat{\nu}_{i'j'}^r G_{jj'}^r(\boldsymbol{\mu}) |(G^r(\boldsymbol{\mu}))^{-1}| \right) \frac{\partial v}{\partial x_j} d\Omega,$$

$$\mathcal{B}(w, v; \boldsymbol{\mu}) = \sum_{r=1}^R \int_{\Omega^r} V_i \frac{\partial w}{\partial x_i} \left( G_{ii'}^r(\boldsymbol{\mu}) |(G^r(\boldsymbol{\mu}))^{-1}| \right) v d\Omega,$$

$$\mathcal{F}(v; \boldsymbol{\mu}) = \sum_{r=1}^R \int_{\Omega^r} \left( \hat{u} |(G^r(\boldsymbol{\mu}))^{-1}| \right) v d\Omega,$$

$$\mathcal{S}(w, v; \boldsymbol{\mu}) = \sum_{r=1}^R \sum_{K \in \mathcal{T}_h^r} \delta_K \int_K V_i \frac{\partial w}{\partial x_i} \left( G_{ii'}^r(\boldsymbol{\mu}) G_{jj'}^r(\boldsymbol{\mu}) |(G^r(\boldsymbol{\mu}))^{-1}| \right) \frac{\partial v}{\partial x_j} V_j dK,$$

$$\mathcal{G}(v; \boldsymbol{\mu}) = \sum_{r=1}^R \sum_{K \in \mathcal{T}_h^r} \delta_K \int_K \hat{u} V_i \frac{\partial v}{\partial x_i} \left( G_{ii'}^r(\boldsymbol{\mu}) |(G^r(\boldsymbol{\mu}))^{-1}| \right) dK,$$

for  $1 \leq i, j \leq 2$ ,  $r = 1, \dots, R$  and  $\hat{\nu}_{i,j}^r = \nu \delta_{i,j}$ .

The *transformation tensors* for the bilinear forms are defined as follows:

$$\nu_{ij}^r(\boldsymbol{\mu}) = G_{ii'}^r(\boldsymbol{\mu}) \hat{\nu}_{i'j'}^r G_{jj'}^r(\boldsymbol{\mu}) |(G^r(\boldsymbol{\mu}))^{-1}|, \quad 1 \leq i, j \leq 2, \quad r = 1, \dots, R,$$

$$\lambda_{ij}^r(\boldsymbol{\mu}) = G_{ii'}^r(\boldsymbol{\mu}) G_{jj'}^r(\boldsymbol{\mu}) |(G^r(\boldsymbol{\mu}))^{-1}| = \frac{\nu_{ij}^r}{\nu}, \quad 1 \leq i, j \leq 2, \quad r = 1, \dots, R,$$

where  $\nu$  is the constant diffusivity in the reference subdomains. For the linear forms we define:

$$\chi_i^r(\boldsymbol{\mu}) = G_{ii'}^r(\boldsymbol{\mu}) |(G^r(\boldsymbol{\mu}))^{-1}|, \quad 1 \leq i \leq 2, \quad r = 1, \dots, R. \quad (41)$$

Furthermore, we may define:

$$\sigma^{q(i,j,r)}(\boldsymbol{\mu}) = \nu_{ij}^r(\boldsymbol{\mu}), \quad \mathcal{A}^{q(i,j,r)}(w, v) = \int_{\Omega^r} \frac{\partial w}{\partial x_i} \frac{\partial v}{\partial x_j} d\Omega,$$

$$\Phi^{s(i,r)}(\boldsymbol{\mu}) = \chi_i^r(\boldsymbol{\mu}), \quad \mathcal{B}^{s(i,r)}(w, v) = \int_{\Omega^r} V_i \frac{\partial w}{\partial x_i} v, \quad d\Omega, \quad (42)$$

$$\Upsilon^{q(i,j,r)}(\boldsymbol{\mu}) = \lambda_{ij}^r(\boldsymbol{\mu}), \quad \mathcal{S}^{q(i,j,r)}(w, v) = \sum_{K \in \mathcal{T}_h^r} \delta_K \int_K V_i \frac{\partial w}{\partial x_i} \frac{\partial v}{\partial x_j} V_j dK, \quad (43)$$

$$\mathcal{G}^{s(i,r)}(v) = \sum_{K \in \mathcal{T}_h^r} \delta_K \int_K \hat{u} V_i \frac{\partial v}{\partial x_i} dK,$$

for  $1 \leq i, j \leq 2$ ,  $r = 1, \dots, R$ , with  $q$  and  $s$  “condensed” indexes for combinations of  $i, j, r$  and  $i, r$ . We can now apply the affine decomposition:

$$\mathcal{A}(\sigma(\boldsymbol{\mu}), w, v) = \sum_{q=1}^{Q^a} \sigma^q(\boldsymbol{\mu}) \mathcal{A}^q(w, v), \quad \mathcal{B}(\Phi(\boldsymbol{\mu}), w, v) = \sum_{s=1}^{Q^b} \Phi^s(\boldsymbol{\mu}) \mathcal{B}^s(w, v),$$

$$\mathcal{S}(\Upsilon(\boldsymbol{\mu}), w_N, v) = \sum_{q=1}^{Q^a} \Upsilon^q(\boldsymbol{\mu}) \mathcal{S}^q(w_N, v), \quad \mathcal{G}(\Phi(\boldsymbol{\mu}), v) = \sum_{s=1}^{Q^b} \Phi^s(\boldsymbol{\mu}) \mathcal{G}^s(v),$$

where  $\max(Q^a) = 2 \times 2 \times R$  and  $\max(Q^b) = 2 \times R$ .

The reduced basis approximation of the stabilized state equation in the reference domain  $\Omega$  reads: *find*  $w_N(\boldsymbol{\mu}) \in W_N$  *such that*

$$\mathcal{A}(w_N, v; \boldsymbol{\mu}) + \mathcal{B}(w_N, v; \boldsymbol{\mu}) + \mathcal{S}(w_N, v; \boldsymbol{\mu}) = \mathcal{F}(v; \boldsymbol{\mu}) + \mathcal{G}(v; \boldsymbol{\mu}), \quad \forall v \in W_N.$$

## 7.2 Parametrized adjoint equation

From the weak formulation of the adjoint problem (10), in the reference domain, we have:

$$\mathcal{B}^{ad}(p, v; \boldsymbol{\mu}) = \sum_{r=1}^R \int_{\Omega^r} V_i \frac{\partial v}{\partial x_i} \left( G_{ii'}^r(\boldsymbol{\mu}) |(G^r(\boldsymbol{\mu}))^{-1}| \right) p \, d\Omega,$$

$$\mathcal{F}^{ad}(v; \boldsymbol{\mu}) = \sum_{r=1}^R \int_{\Omega^r} \left( \chi_D \hat{g} (\hat{g} \hat{w} - \hat{z}_d) |(G^r(\boldsymbol{\mu}))^{-1}| \right) v \, d\Omega,$$

$$\mathcal{S}^{ad}(p, v; \boldsymbol{\mu}) = \sum_{r=1}^R \sum_{K \in \mathcal{T}_h^r} \delta_K \int_K V_i \frac{\partial p}{\partial x_i} \left( G_{ii'}^r(\boldsymbol{\mu}) G_{jj'}^r(\boldsymbol{\mu}) |(G^r(\boldsymbol{\mu}))^{-1}| \right) \frac{\partial v}{\partial x_j} V_j \, dK,$$

$$\mathcal{G}^{ad}(v; \boldsymbol{\mu}) = - \sum_{r=1}^R \sum_{K \in \mathcal{T}_h^r} \delta_K \int_K \chi_D \hat{g} (\hat{g} \hat{w}_N - \hat{z}_d) \left( V_i \frac{\partial v}{\partial x_i} \right) \left( G_{ii'}^r(\boldsymbol{\mu}) |(G^r(\boldsymbol{\mu}))^{-1}| \right) dK,$$

$$\mathcal{H}^{ad}(v; \boldsymbol{\mu}) = - \sum_{r=1}^R \sum_{K \in \mathcal{T}_h^r} \delta_K \int_K \chi_D \hat{g}^2 \left( V_i \frac{\partial \hat{w}_N}{\partial x_i} \right) \left( G_{ii'}^r(\boldsymbol{\mu}) |(G^r(\boldsymbol{\mu}))^{-1}| \right) v \, dK.$$

We introduce:

$$\Phi^{s(i,r)}(\boldsymbol{\mu}) = \chi_i^r(\boldsymbol{\mu}), \quad \mathcal{B}_{ad}^{s(i,r)}(p, v) = \int_{\Omega^r} V_i \frac{\partial v}{\partial x_i} p \, d\Omega,$$

$$\mathcal{S}_{ad}^{q(i,j,r)}(p_N, v) = \sum_{K \in \mathcal{T}_h^r} \delta_K \int_K V_i \frac{\partial p_N}{\partial x_i} \frac{\partial v}{\partial x_j} V_j \, dK, \quad \forall v \in Z_N,$$

$$\mathcal{G}_{ad}^{s(i,r)}(v) = - \sum_{K \in \mathcal{T}_h^r} \delta_K \int_K \chi_D \hat{g} \left( \hat{g} \hat{w}_N - \hat{z}_d \right) \left( V_i \frac{\partial v}{\partial x_i} \right) dK,$$

$$\mathcal{H}_{ad}^{s(i,r)}(v) = - \sum_{K \in \mathcal{T}_h^r} \delta_K \int_K \chi_D \hat{g}^2 \left( V_i \frac{\partial w_N}{\partial x_i} \right) v dK,$$

for  $1 \leq i, j \leq 2$ ,  $1 \leq r \leq R$ , where  $\chi_i^r(\boldsymbol{\mu})$  is defined by (41).

By definitions, we have:

$$\mathcal{B}^{ad}(\Phi(\boldsymbol{\mu}), p, v) = \sum_{s=1}^{Q^b} \Phi^s(\boldsymbol{\mu}) \mathcal{B}_{ad}^s(p, v), \quad \mathcal{S}^{ad}(\Upsilon(\boldsymbol{\mu}), p, v) = \sum_{q=1}^{Q^a} \Upsilon^q(\boldsymbol{\mu}) \mathcal{S}_{ad}^q(p, v),$$

$$\mathcal{G}^{ad}(\Phi(\boldsymbol{\mu}), v) = \sum_{s=1}^{Q^b} \Phi^s(\boldsymbol{\mu}) \mathcal{G}_{ad}^s(v), \quad \mathcal{H}^{ad}(\Phi(\boldsymbol{\mu}), v) = \sum_{s=1}^{Q^b} \Phi^s(\boldsymbol{\mu}) \mathcal{H}_{ad}^s(v),$$

where  $\Upsilon^q(\boldsymbol{\mu})$  e  $\Phi^s(\boldsymbol{\mu})$  are respectively defined in (43) and (42).

The reduced basis approximation of the stabilized adjoint equation in the reference domain  $\Omega$  is: *find*  $p_N(\boldsymbol{\mu}) \in Z_N$  such that

$$\mathcal{A}(p_N, v) + \mathcal{B}^{ad}(p_N, v) + \mathcal{S}^{ad}(p_N, v) = \mathcal{F}^{ad}(v) + \mathcal{G}^{ad}(v) + \mathcal{H}^{ad}(v) \quad \forall v \in Z_N.$$

At this point we solve a *parametrized optimal control problem*.

### 7.3 Geometrical sensitivity analysis results

We fix the chimneys emission rates ( $u_1 = 20\%$  of  $u_{tot} = 2700$  g/s,  $u_2 = 5\%$ , then  $u_3 = 75\%$ ) and the wind velocity ( $\mathbf{V} = (2.5, 0)$ ), considering as variable parameters the geometrical quantities only. With an adaptive procedure [14], we find 35 basis functions.

We report in Fig.6 the result of the analysis for the parametrized domain illustrated in Fig.5. We note that, fixing  $C_3$  (i.e. the position of the upper chimney), pollutant concentration over the city decreases when  $C_2$  goes from 0.1 to 1.3 Km, while for  $1.3 \leq C_2 \leq 2.9$  there are no important variations. This is due to the fact that for  $C_2 \geq 1.3$  the city is outside of the lower chimney emission cone. If we keep constant  $C_2$ , and therefore the position of the lower chimney, we note that pollutant concentration over the city increases rapidly till it reaches its maximum around  $C_3 = 1$ , then it decreases till  $C_3 = 2.9$ . A possible explanation of this behavior is that for  $C_3 = 0.1$  the city is only partially under the pollutant wake, for  $C_3 = 1$  it is totally inside of it, while when  $C_3 \geq 1$  the city sets gradually outside of the emission cone.

Summing up the results, moving the lower chimney towards the lower domain edge, beyond  $C_2 = 1.3$ , does not imply any advantages, while moving the upper chimney from  $C_3 = 1$  to  $C_3 = 2.9$  causes a pollution reduction of around 80%.

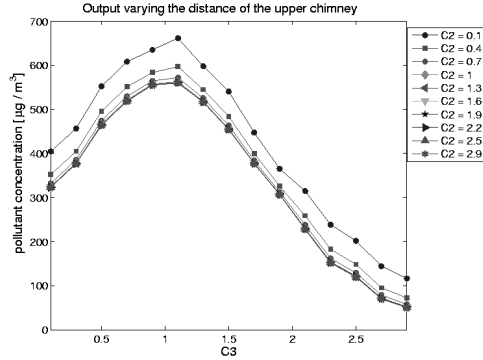


Figure 6: Variations of pollutant concentration (in  $\mu\text{g}/\text{m}^3$ ) over the city when the upper ( $C_3$ ) and lower ( $C_2$ ) chimney positions change.

#### 7.4 Sensitivity analysis applied to control problem

The choice of geometrical inputs allows us to study the state variable sensitivity to domain variations, to know how the pollutant concentration over the observation area varies according to the geometrical changes. We want now to exploit this state variable sensitivity in solving the control problem, in order to maximize the factory productivity level while keeping the pollution level under the fixed threshold. With our model we can find the best positions for the upper and lower chimneys.

To that purpose we modify the iterative method adopted to solve the control problem. Starting always from an initial value for control variable  $u_0$ , we solve both the state and adjoint equations. Once  $p$  is known, we check if the stopping criterium (8) is satisfied. At every iterative step in which the adjoint variable does not satisfy the stopping criterium, instead of starting directly an iterative process on control variable  $u$ , we try first to fulfill the criterium by simply varying the positions of upper and lower chimneys. If we cannot satisfy it just by modifying the geometry, then we update control variable value adopting the steepest descent method (7). In this way we minimize the number of iterations on  $u$  and therefore we maximize the productivity, because chimneys emissions decrease at every step (since  $u^{k+1} = u^k - \tau \delta u^k$ ). Fig.7 illustrates the flow diagram of this new method for solving the control problem.

Six input parameters are used for this test problem, comprising the emission rates of the first two chimneys and the geometrical parameters, that is  $\mu = \{u_1, u_2, C_1, C_2, C_3, C_4\}$ , ranging in the set  $\mathcal{D} = [0, 2700] \times [0, 2700] \times [0.1, 2.9] \times [0.1, 2.9] \times [0.1, 2.9] \times [0.1, 2.9]$ .

We notice that for  $N = 80$  of basis functions, the reduced basis solution of the control problem is a “good” approximation of the finite element solution, i.e. the mean  $H^1$ -error for random inputs is about  $10^{-5}$ . To verify that the control

problem solved with the finite element method and the one solved with the reduced basis method converged to the same solution, we compute the two errors  $\varepsilon_u$  and  $\varepsilon_J$  for a certain number of random inputs. Imposing  $tol = 10^{-7}$ , we find that the order of magnitude for  $\varepsilon_u$  is  $10^{-5}$ , while for  $\varepsilon_J$  is  $10^{-10}$ .

As an illustrative example, we consider the following initial configuration: up-

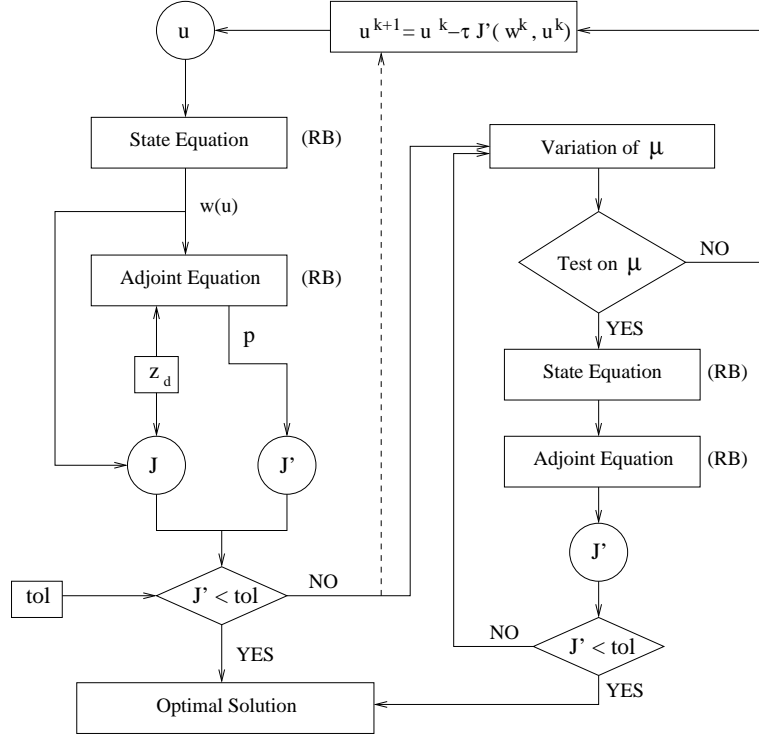


Figure 7: Flow diagram of the iterative process to solve control problem combined with sensitivity analysis.

per chimney emitting at 30% of  $u_{tot} = 2700$  g/s and central chimney emitting at 40%, in unstable air conditions. For  $tol = 10^{-7}$ , the iterative method converges after four iterations on  $u$  to the optimal solution: the upper chimney switched off, the central one emitting at 18.3% of  $u_{tot}$  and the lower one at 29.83%, with  $C_2 = 0.4$  Km and  $C_3 = 2.9$  Km. The control problem without sensitivity analysis has another solution:  $u_1 = 3.55\%$ ,  $u_3 = 28.66\%$  and central chimney switched off, which means that the productivity is reduced by 15.92% on total  $u_{tot}$ . In this case,  $\varepsilon_J = 2 \cdot 10^{-10}$  and  $\varepsilon_u = 4.4 \cdot 10^{-5}$ .

## 8 Concluding remarks

By adopting the reduced basis method for the solution of both state and adjoint equations at every steps of the iterative method used to solve the optimal control

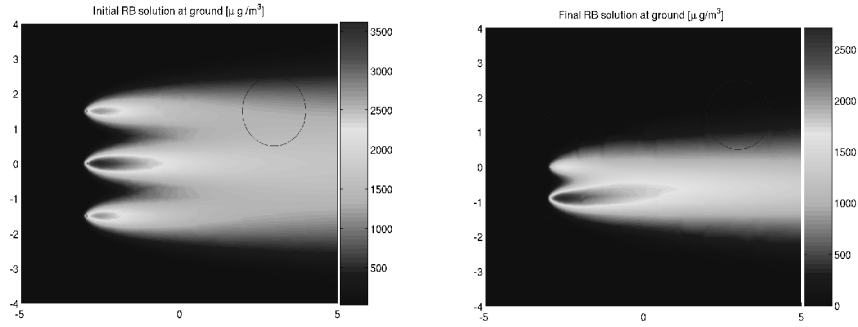


Figure 8: Geometrical Input: initial reduced basis solution (right) and final reduced basis solution (left) of state equation. Pollutant concentration is in  $[\mu\text{g}/\text{m}^3]$ .

problem may yield significant advantages from a computational point of view. The reduced basis method shows great versatility. In fact we analyzed different input parameter classes: *control input* - in our application this kind of input is related to the productivity level of the industrial plant, and so to regulations and economical and commercial factors; *physical input* - this kind of input allows us to take into account meteorologic conditions and characteristics of the area where the factory and the city lie; *geometrical input* - in order to consider the position of the city with respect to the industrial chimneys. With all these different parametrizations we are able to solve the control problem from a global and decisional point of view, considering, at the same time, several aspects of the same problem.

## Acknowledgements

We acknowledge Dott. Ing. L. Dedé (MOX-Politecnico di Milano) for his kind collaboration and great help. We are also sincerely grateful to Prof. A.T. Patera and Dr. M. Grepl (MIT) for important suggestions, remarks and insights.

## References

- [1] M. Barrault, Y. Maday, N.C. Nguyen, A.T.Patera. An “empirical interpolation” method: application to efficient reduced-basis discretization of partial differential equations. *C. R. Acad. Sci. Paris, Analyse Numerique, Serie I* (2005) **339**, 667–672.



- [2] R. Becker, H. Kapp, R. Rannacher. Adaptive finite elements methods for optimal control of partial differential equations: basic concepts. *SIAM J. Control Opt.* (2000) **39**, No.1.
- [3] L. Dedè, A. Quarteroni. *Optimal control and numerical adaptivity for advection-diffusion equations. M2AN* (2005) **39** No. 5, 1019–1040.
- [4] G. Finzi, G. Pirovano, M. Volta. *Gestione della Qualità dell’Aria. Modelli di Simulazione e Previsione.* McGraw-Hill, Milano, 2001.
- [5] M. Grepl. *Reduced Basis Approximation and A posteriori Error Estimation for Parabolic Partial Differential Equations.* Phd thesis, MIT, Massachusetts Institute of Technology, 2005.
- [6] K. Ito, S.S. Ravindran. A reduced-order method for simulation and control of fluid flow. *Journal of Computational Physics* (1998) **143**, No.2, 403–425.
- [7] K. Ito, S.S. Ravindran. A reduced basis method for control problems governed by PDEs. *International Series of Numerical Mathematics* (1998) **126**, Birkäuser Verlag, 153–168.
- [8] K. Ito, S.S. Ravindran. Reduced basis methods for optimal control of unsteady viscous flows. *International Journal of Computational Fluid Dynamics* (2001) **15**, 97–113.
- [9] J.L. Lions. *Optimal Control of Systems Governed by Partial Differential Equations.* Springer-Verlag, NY, 1971.
- [10] N.C. Nguyen. *Reduced Basis Approximation and A Posteriori Error Bounds for Nonaffine and Non-linear Partial Differential Equations: Application to Inverse Analysis.* PhD Thesis, Singapore-MIT Alliance, National University of Singapore, 2005.
- [11] C. Prud’homme, D. V. Rovas, K. Veroy, L. Machiels, Y. Maday, A. T. Patera, G. Turinici. Reliable real-time solution of parametrized partial differential equations: reduced-basis output bound methods. *J. Fluids Engineering* (2002) **172**, 70–80.
- [12] A. Quarteroni, G. Rozza, L. Dedè, A. Quaini. Numerical approximation of a control problem for advection-diffusion processes. In *System Modeling and Optimization*, Proceedings of IFIP Conference 2005, Turin, Italy Springer, NY, 2006.
- [13] A. Quarteroni, A. Valli. *Numerical Approximation of Partial Differential Equations.* Springer-Verlag, Berlin, 1994.
- [14] G. Rozza. Reduced basis methods for elliptic equations in sub-domains with a posteriori error bounds and adaptivity. *Applied Numerical Mathematics* (2005), **55**, No.4, 403–424.

- [15] G. Rozza. *Shape Design by Optimal Flow Control and Reduced Basis Techniques: Applications to Bypass Configurations in Haemodynamics*. PhD Thesis No.3400, EPFL, Ecole Polytechnique Fédérale de Lausanne, 2005.